TRANSPORT AND ESCAPE OF WATER: TOWARD A MORE COMPLETE INTERPRETATION WITH TGO NOMAD AND MAVEN NGIMS.

S. W. Stone, G. L. Villanueva, G. Liuzzi, M. Benna, P. R. Mahaffy, M. K. Elrod, *NASA Goddard Space Flight Center, Greenbelt, MD, USA*, **R. V. Yelle,** *Lunar and Planetary Laboratory, University of Arizona, Tucson, AZ, USA*.

Introduction

The present-day transport, destruction, and subsequent loss to space of H_2O in the Martian atmosphere has important implications for our understanding of the evolution of the Martian atmosphere and climate through time.[1] On Earth, most H_2O is trapped relatively close to the surface by an efficient hygropause. In contrast, on Mars the hygropause is often transgressed by significant amounts of H_2O transported vertically from the lower atmosphere around perihelion, corresponding to southern hemisphere summer, during regional dust storms which occur every Martian year, and during global dust storms which occur roughly every ten years.[2–8] A portion of this H_2O progresses into the upper atmosphere, where it is quickly destroyed by ion-neutral reactions to produce H that can escape to space.[7, 9] This relatively rapid transport of H into the upper atmosphere in the form of H_2O is supplemented by the steady flow of H_2. H_2 is produced in the lower atmosphere by the photolysis of H_2O and subsequent odd-hydrogen reactions. The H_2 is then transported vertically *via* diffusion past the hygropause and into the thermosphere, where it is destroyed by ion-neutral reactions in a manner similar to H_2O, producing H.

The imprint of escape on the atmosphere is observed in the isotope ratios of escaping elements. For example, the preferential escape of H over heavier D *via* the Jeans mechanism[10, 11] leads to the enrichment of the atmosphere in D relative to H.[12–14] A number of other processes are responsible for isotopic fractionation in the atmosphere, including preferential condensation of HDO relative to H_2O and the distinct photolysis rates of molecular isotopologues.[13–17] Using measurements of the H_2O abundance and various isotope ratios in the lower, middle, and upper atmosphere, this work aims to construct a more complete understanding of the transport of H_2O into the upper atmosphere, its condensation and destruction, and its escape to space.

Methods

Upper atmospheric H_2O densities are calculated from Mars Atmosphere and Volatile EvolutioN (MAVEN) Neutral Gas and Ion Mass Spectrometer (NGIMS) ion measurements assuming photochemical equilibrium (Figure 1).[7] NGIMS measurements of atmospheric H_2O at mass per charge (m/z) 18 are not possible due to

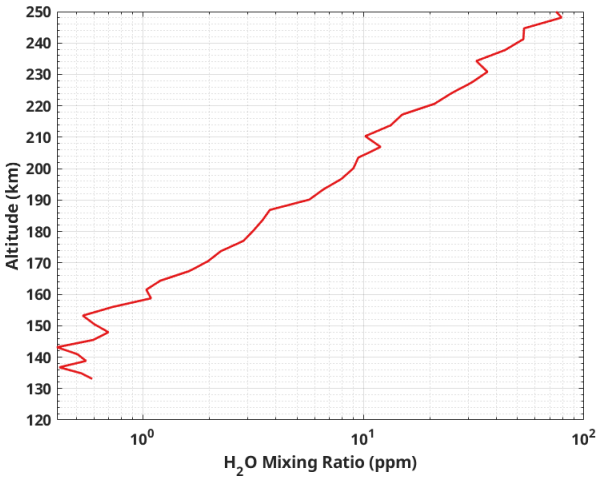

Figure 1: The H_2O abundance calculated from MAVEN NGIMS data on a single orbit. In this region of the atmosphere, the mixing ratio increases with height due to diffusive separation.

background signal of H_2O synthesized from reactive atmospheric species once inside the instrument. Thus, the H_2O abundance is calculated from NGIMS ion measurements using photochemical equilibrium calculations based on the production and loss reactions of H_3O^+:

$$\begin{aligned} H_3O^+ + e^- &\xrightarrow{\alpha_1} OH + H + H \\ &\xrightarrow{\alpha_2} H_2O + H \\ &\xrightarrow{\alpha_3} OH + H_2 \\ &\xrightarrow{\alpha_4} O + H_2 + H \end{aligned}$$

$$HCO^+ + H_2O \xrightarrow{k_1} H_3O^+ + CO$$

$$H_2O^+ + H_2O \xrightarrow{k_2} H_3O^+ + OH$$

This allows us to construct a simple equation for the H_2O abundance,

$$[H_2O] = (\alpha_1 + \alpha_2 + \alpha_3 + \alpha_4)\,\frac{[H_3O^+][e^-]}{k_1[HCO^+] + k_2[H_2O^+]}.$$

The species on the righthand side of the equation are measured by the ion mode of NGIMS and the reaction rates are obtained from the University of Manchester

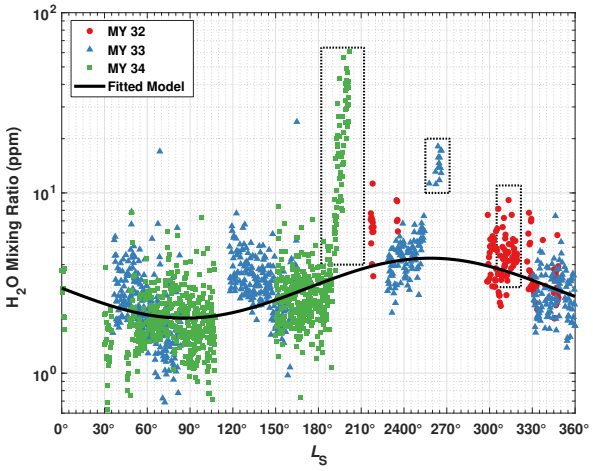

Figure 2: Seasonal Variation of H_2O in the upper atmosphere of Mars as observed by MAVEN NGIMS.[7] The H_2O abundance in the upper atmosphere peaks during southern summer (L_S ~270°) and significant enhancements in the H_2O abundance are observed during dust storms (black boxes), both regional (MYs 32 and 33) and global (MY 34). The black line is a sine fit to the data, excluding the dust storms.

Institute of Science and Technology (UMIST) Database for Astrochemistry (UDfA).[18]

ExoMars Trace Gas Orbiter (TGO) Nadir and Occultation for MArs Discovery (NOMAD) measurements of H_2O, HDO, and water ice in the lower and middle atmosphere are obtained using the Solar Occultation (SO) channel in the infrared between wavelengths of 2.2 µm and 4.3 µm.[14, 19] During an occultation, the atmosphere is sensed by pointing the instrument at the Sun and measuring the absorption of solar photons by molecules and aerosols along the tangential line of sight. Such measurements are obtained at increasing or decreasing altitudes along the dawn or dusk terminator of Mars to probe the vertical variation of the absorbing molecules and aerosols. The NOMAD SO channel is an echelle spectrometer with an acousto-optical tunable filter (AOTF) which limits the observed signal to a single diffraction order. Calibration of the instrument through characterization of the AOTF response functions, grating parameters, and instrument line shape function is necessary for accurate interpretation of spectral features. Detailed information on these quantities is currently under review.[20] The H_2O absorption features used here are the bands in the 2.2 µm and 3.3 µm region (NOMAD SO diffraction orders 133 to 170). For HDO, the ν_1 band at 3.7 µm is used (orders 119 to 121). Retrieval of molecular abundances from the NOMAD occultations is performed by the Planetary Spectrum Generator (PSG) using a layer-by-layer and line-by-line method in a spherical refractive geometry.[21] Molecular line lists are obtained from the HITRAN-2020 database and PSG uses the latest line broadening coefficients for H_2O and HDO in a CO_2 atmosphere.[22–24] The *a priori* atmosphere used by PSG is generated by the Global Environmental Multiscale general circulation model for Mars (GEM-Mars).[25]

Results and Discussion

The combination of the TGO NOMAD and MAVEN NGIMS data sets enables a more complete interpretation of the transport of H_2O through the atmosphere of Mars and its eventual escape as H and O. The H_2O abundance can now be retrieved nearly continuously from the lower atmosphere to the thermosphere. In addition, various isotope ratios can be retrieved from the two data sets in the lower, middle, and upper atmosphere, supporting the study of the relative importance of condensation, photolysis, and escape in the determination of these ratios in the atmosphere over various timescales.

Using NGIMS and NOMAD data spanning several Mars years, the seasonal variation of the H_2O abundance in the upper atmosphere is obtained (Figures 2–4). The NGIMS data have indicated that more H_2O is transported into the upper atmosphere during southern summer than during northern summer and that regional and global dust storms rapidly loft even more H_2O into the upper atmosphere (Figures 2 and 3).[7] Similarly, these variations are observed in the lower and middle atmosphere using NOMAD (Figure 4).[14] Once combined with NOMAD retrievals of HDO and water ice particle size,[14, 19] these H_2O measurements are powerful indicators of the role of condensation in the fractionation of hydrogen isotopes in water at altitudes between 10 km and 60 km. Isotopic fractionation of H_2O also occurs through its photolytic destruction in the middle atmosphere.[13] Here, 1D photochemical modeling and NGIMS H_2O abundances in the lower thermosphere can aid in our understanding of the importance of photolysis and ion-neutral reactions with respect to escape and the long term evolution of the D/H ratio on Mars. Additional context may be provided by the isotope ratios measured by NGIMS in the upper atmosphere. Finally, observations in the UV made by the Imaging Ultraviolet Spectrograph (IUVS) on MAVEN track the abundance and variation of escaping H and D, providing a view of the end result of these processes.[26, 27]

References

[1] Haberle, et al. (Eds.). **2017**. *The Atmosphere and Climate of Mars*. Cambridge University Press. [2] Chaffin, et al. **2014**. Geophys. Res. Lett., *41*(2), 314–320. [3] Clarke, et al. **2014**. Geophys. Res. Lett., *41*(22), 8013–8020. [4] Chaffin, et al. **2017**. Nat. Geosci., *10*(3), 174–178. [5] Vandaele, et al. **2019**. Nature, *568*(7753), 521–525. [6] Fedorova, et al. **2020**. Science, *367*(6475),

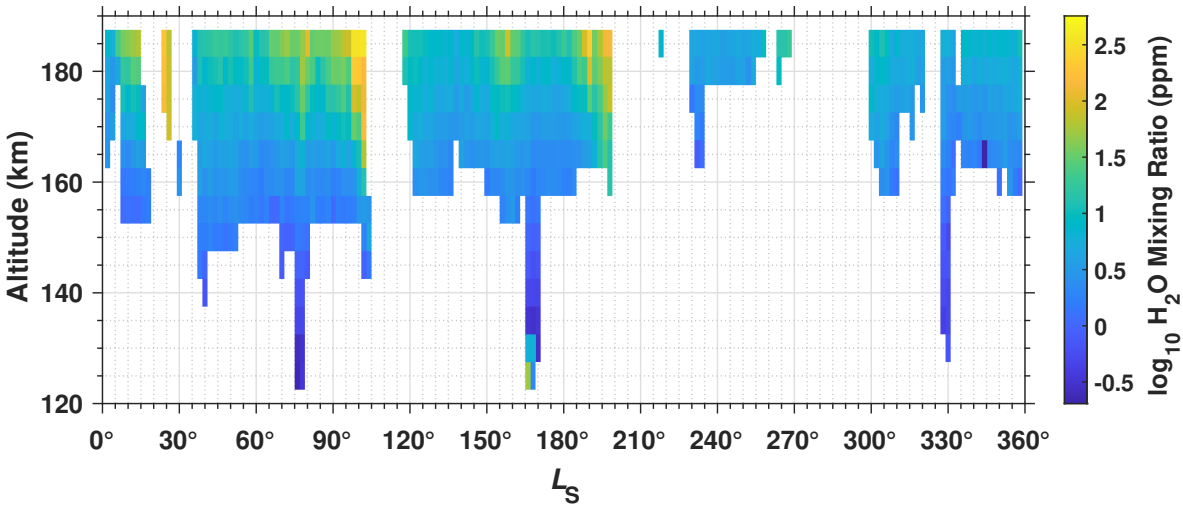

Figure 3: Seasonal variability of the H_2O in the upper atmosphere of Mars as calculated from the MAVEN NGIMS data.

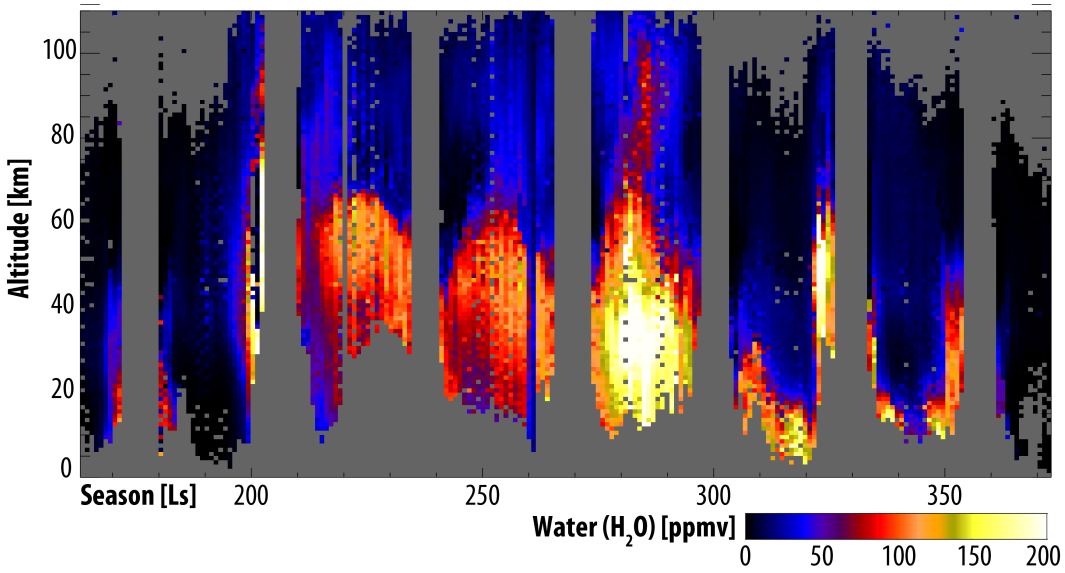

Figure 4: Seasonal variability of the H_2O abundance in the southern hemisphere as measured by TGO NOMAD. See reference [14].

297–300. [7] Stone, et al. **2020**. Science, *370*(6518), 824–831. [8] Chaffin, et al. **2021**. Nat. Astron., *5*, 1036–1042. [9] Krasnopolsky. **2019**. Icarus, *321*, 62–70. [10] Johnson, et al. **2008**. Space Sci. Rev., *139*(1-4), 355–397. [11] Gronoff, et al. **2020**. J. Geophys. Res. Space Phys., *125*(8). [12] Webster, et al. **2013**. Science, *341*(6143), 260–263. [13] Alday, et al. **2021**. Nat. Astron., *5*(9), 943–950. [14] Villanueva, et al. **2021**. Sci. Adv., *7*(7), eabc8843. [15] Bertaux, et al. **2001**. J. Geophys. Res. Planets, *106*(E12), 32879–32884. [16] Montmessin, et al. **2005**. J. Geophys. Res. Planets, *110*, E03006. [17] Villanueva, et al. **2015**. Science, *348*(6231), 218–221. [18] McElroy, et al. **2013**. Astron. & Astrophys., *550*, A36. [19] Liuzzi, et al. **2020**. J. Geophys. Res. Planets, *125*(4). [20] Villanueva, et al. **2022**. Geophys. Res. Lett., under review. [21] Villanueva, et al. **2018**. J. Quant. Spectrosc. Radiat. Transf., *217*, 86–104. [22] Gordon, et al. **2022**. J. Quant. Spectrosc. Radiat. Transf., *277*, 107949. [23] Devi, et al. **2017**. J. Quant. Spectrosc. Radiat. Transf., *203*, 158–174. [24] Régalia, et al. **2019**. J. Quant. Spectrosc. Radiat. Transf., *231*, 126–135. [25] Neary, et al. **2018**. Icarus, *300*, 458–476. [26] Chaffin, et al. **2018**. J. Geophys. Res. Planets, *123*(8), 2192–2210. [27] Mayyasi, et al. **2019**. J. Geophys. Res. Space Phys., *124*(3), 2152–2164.